Activation of Glomerular Basement Membrane–Specific B Cells in the Renal Draining Lymph Node after T Cell–Mediated Glomerular Injury

Julie Robertson,* Jean Wu,* Jon Arends,* Cindy Zhou,* John McMahon,† Lisa Torres,* and Ya-Huan Lou*

**Department of Diagnostic Sciences, Dental Branch, and the †Department of Integrative Biology and Pharmacology, Medical School, University of Texas Health Science Center at Houston, Houston, Texas*

Linear binding of IgG to the glomerular basement membrane (GBM) is the hallmark of anti-GBM glomerulonephritis (GN). However, the precise mechanism by which diverse autoantibodies to GBM are induced in GN has not been determined. It was demonstrated previously that a single T cell epitope pCol(28–40) derived from collagen IV α3 chain not only induced severe GN in Wistar Kyoto rats but also triggered a diversified anti-GBM antibody response through "B cell epitope spreading." In this study, an expansion of T and B cells in the renal draining lymph node (RDLN) of diseased animals after glomerular injury was observed. RDLN was demonstrated to be the location of GBM-specific B cell activation. First, B cells from RDLN of pCol(28–40)-immunized rats produced *in vitro* anti-GBM antibodies and antinuclear antibodies. Second, B cells specific to the peptidic B cell epitope in pCol(28–40) were absent among expanding B cells in RDLN. Those findings provided a unique opportunity to track activation of diverse GBM-specific B cells in RDLN. Expression of B lymphocyte-induced maturation protein-1, which is involved in differentiation of plasma cells, in B cells of RDLN was detected and further elevated only after T cell–mediated prominent glomerular injury (day 19). This was supported by the fact that anti-GBM antibodies became detectable only after day 20. Those results suggest that T cell–mediated glomerular injury may trigger *de novo* internal immunization of autoantigens released from damaged GBM, which further leads to activation of a group of GBM-specific B cells in RDLN.

J Am Soc Nephrol 16: 3256–3263, 2005. doi: 10.1681/ASN.2005040421

Production of autoantibodies to diverse autoantigens, which are usually clustered or physically associated, is a characteristic of human autoimmune diseases (1). It is well exemplified in anti–glomerular basement membrane (GBM) glomerulonephritis (GN) or Goodpasture's syndrome. Autoantibodies from patients with GN react with conformational B cell epitopes of diverse GBM proteins, which include the NC domain of collagen IV α3 chain (Col4α3NC1), different chains of type IV collagen, collagen domains and S7 domains of type IV collagen, and other noncollagen components (2–5). In addition to their pathologic roles in tissue damage, the presence of anti-GBM autoantibody is one of the most important diagnostic indices for this disease. However, the precise mechanism by which autoantibodies to GBM are induced in GN has not been determined.

The mechanisms of the B cell tolerance and production of autoantibodies have been studied at several levels. First, several signal pathways have been revealed to participate in B cell selection/tolerance, especially in T-independent responses (6–8). However, those mechanisms cannot explain diversified autoantibody responses to clustered target antigens as seen in anti-GBM disease. Second, BcR transgenic mice have been a valuable tool in the study of B cell tolerance to a special autoantigen, because "autoreactive" B cells can be tracked easily (9,10). Those genetically manipulated animals have been instrumental in our understanding of B cell tolerance and activation. Obviously, mono-specific B cells in transgenic models may not be suitable for study on diversified autoantibody responses as seen in anti-GBM disease.

Many studies suggest that B cell tolerance in many cases is T cell dependent. It has been reported in several animal models that a pathogenic T cell epitope triggers production of diverse autoantibodies, or "B cell epitope spreading" (11–14). B cell epitope spreading also has been observed in our rat model for T cell–mediated anti-GBM GN (15). A single pathogenic T cell epitope pCol(28–40) derived from collagen 4α3 chain (Col4α3) not only induces severe GN but also elicits an autoantibody response to diverse GBM antigens (16–18). It has been postulated that the T cells, activated by a pathogenic T cell epitope, may provide help to a population of autoreactive B cells, which present the same T cell epitope of endogenous autoantigens during B cell epitope spreading (19,20). However, it has been difficult to verify this hypothesis in normal animals because of lack of a model in which diverse autoreactive B cell populations can be tracked for analysis.

In this study, we identified the renal draining lymph node (RDLN) as the location for activation of autoreactive B cells after T

Received April 21, 2005. Accepted July 22, 2005.

Published online ahead of print. Publication date available at www.jasn.org.

Address correspondence to: Dr. Ya-Huan Lou, Department of Diagnostic Sciences, Dental Branch, University of Texas Health Science Center at Houston, 6516 M.D. Anderson Blvd, Houston, TX 77030. Phone: 713-500-4059; Fax: 713-500-4416; E-mail: yahuan.lou@uth.tmc.edu

ISSN: 1046-6673/1611-3256

cell–mediated glomerular damage in our anti-GBM GN model. Thus, diverse autoreactive B cell populations can be tracked and their activation can be studied at cellular and molecular levels. Our model provides a unique chance to investigate how the GBM-specific B cells are activated.

Materials and Methods

Antigen Preparation and Induction of GN

Peptides were synthesized on an automatic peptide synthesizer, AMS 422 (Gilson, Middleton, WI) using Fmoc chemistry and were purified by a reverse-phase C18 column on preparative HPLC (Water, Millford, MA). Purified peptides were analyzed by HPLC for purity and by mass spectrometry for the correct sequence. Peptides that exceeded 95% purity were dissolved in milli-Q water at 1 mM concentration and used for immunization or other investigative purposes. Sequences of synthesized peptides are listed in Table 1.

Female Wistar Kyoto (WKY) rats were allowed to acclimate for a minimum of 3 d and were immunized in one hind footpad and at the base of the tail with a peptide (0.125 μmol) emulsified in complete Freund adjuvant (CFA). Rats that were immunized with CFA alone served as controls. GN was evaluated by measurement of proteinuria/albuminuria and examination of renal histopathology (16). Renal tissues fixed in Bouin's solution were used for hematoxylin and eosin staining (16). Glomerular injury score was calculated as the following: [(number of crescentic glomeruli $\times$ 100) + (number of hypercellular glomeruli $\times$ 50)] $\div$ total number of glomeruli.

Investigation of Renal Lymphatic Drainage

Rats were anesthetized with ketamine/xylazine (50/7 mg/kg). A small dorsal incision was made, and the left kidney was exposed through the incision. India ink (tissue culture grade; Sigma, St. Louis, MO) was injected into the external border of the renal cortex using a 20-gauge needle (three sites, 10 μl/site). The animals were allowed to recover and were killed 3 to 12 h later. The RDLN, which was stained by the ink, was identified, and the presence of carbon particles in its cortical area was confirmed under a dissecting microscope.

Isolation of Kidney-Infiltrating Leukocytes

Renal cortex was sliced, placed in a cold DMEM that contained 10% FCS, ground against #100 mesh, and rinsed repeatedly. The passing-through materials included intact glomeruli, fragmented tubules, and single cells. The single cells were separated by a cell constrainer (80 μm) and designated as "interstitial cells." The glomeruli, which were collected from the cell constrainer, were then separated from the tubules by recombination of gravity sediment and low-speed centrifugation (200 rpm for 4 min) (15). The purity of the glomeruli, which was determined under a microscope, was approximately 80 to 85%. The purified glomeruli were incubated further with collagenase IV at 37°C for 30 min with periodic stirring. After the incubation, glomerular fragments were eliminated by low-speed centrifugation (300 rpm for 5 min), and the single cells were collected by a higher speed centrifugation (1000 rpm for 10 min). Those cells were designated as "glomerular cells." Both interstitial cells and glomerular cells were stained for several leukocyte markers, including CD4, CD8, CD11b/c, OX33, and IgG/M, and analyzed with a flow cytometer (FACSCalibur; Becton Dickinson, San Jose, CA).

Flow Cytometry and Immunofluorescence Detection of pCol(28–40)-Specific B Cells

FITC-pCol(28–40) was commercially synthesized through Ahx at the amino terminus of the peptide (Biosynthesis, Lewisville, TX), dissolved in PBS at a concentration of 1 mM (1.8 mg/ml), and kept in the dark. ELISA confirmed that anti-pCol(28–40) antibody bound to FITC-pCol(28–40).

The lymphocytes were adjusted to 5×10^6 cells/ml and fixed in 0.5% paraformaldehyde (PFA) for 5 min. The cells (0.5×10^6 cells) were stained with FITC-pCol(28–40) (10 μM) and PE-labeled mAb OX33 (10 μg/ml) on ice for 30 min. After washing with PBS, the cells were analyzed by a flow cytometer. B cells that were specific to pCol(28–40) were identified as double positive for both pCol(28–40) and OX33. As plasma cells do not express OX33, they were identified as pCol(28–40) single positive cells. FITC-pCol(28–40) is able to bind to MHC class II (RT.1B*l*) on several cell populations such as macrophages at a lower intensity (18). mAb OX6, which reacts with RT.1B*l*, was used to reduce the background.

For immunofluorescence, frozen sections of lymph nodes were briefly fixed in cold acetone for 10 min and washed in cold PBS. The sections were preincubated with OX6 (10 μg/ml) to prevent possible binding of pCol(28–40) to MHC class II, followed by incubation with FITC-pCol(28–40) and PE-OX33 at room temperature. The sections were sealed with a mounting solution and viewed with a confocal microscope.

In Vitro *Antibody Production*

Lymphocytes were isolated from either RDLN or inguinal lymph nodes (ILN). The cells were incubated in a serum-free medium at a cell density of 5×10^6 cell/ml following our previously published method (17). The supernatant of the culture was collected, and IgG concentration was determined by ELISA with a pair of anti-rat IgG antibodies using normal rat IgG as a standard (Southern Biotechnology, Birmingham, AL). The supernatant was dialyzed against 20 mM ammonium carbonate and lyophilized. The dried powder was re-dissolved in sterilized PBS (50 mM, pH 7.2) with 1 mg/ml BSA as a stabilizer, and the IgG concentration was re-measured. The IgG was kept at 4°C with 0.1% sodium azide for subsequent applications.

Detection of Antibody Activity

A previously described ELISA method was applied to detect antibodies to peptides (15). Briefly, plates were coated with 50 μl of peptide of 10 μM in a carbonate buffer (pH 9.5). Serially diluted serum (100 to 800) was added to each well in duplicate. The bound rat IgG antibodies were detected with horseradish peroxidase–labeled goat anti-rat IgG (1:10,000;

Table 1. Peptides pCol(28–40), derivatives used in this study and their immune properties and nephritogenicity

Peptide	Sequence	T Cell Epitope (Restriction)	B Cell Epitope[a]	Nephritogenic
pCol(28–40)	QTTANPACPEGT	Identical (RT.1B*l*)	Identical	Yes
FITC-Ash-pCol(28–40)[b]	FITC-Ash-SQTTANPACPEGT	Identical (RT.1B*l*)	Identical	Yes
pCol(34A)[c]	SQTTANAACPEGT	Altered (RT.1B*l*)	Identical	No

[a]Antibody to this B cell epitope only reacts with the peptide but not with native glomerular basement membrane (GBM).
[b]Used as a probe.
[c]pCol34A, pCol(28–40) with single alanine substitution at position 34.

Southern Biotechnology) using O-phenoldiamine (0.25 mg/ml) as the substrate. The plates were read on an ELISA reader at 490 nm. A similar ELISA was used for detection of anti-GBM antibody using digested GBM proteins (15).

Direct immunofluorescence study was carried out to detect the anti-GBM antibody that bound to GBM *in vivo* (15), using FITC-labeled goat anti-rat IgG or IgM antibodies (1:50; Southern Biotechnology). Indirect immunofluorescence was used to detect antibodies to native GBM. Rat kidney contains a significant amount of Ig, which will also be stained by anti-rat IgG. Such background is not acceptable in the case for detection of a small quantity of rat antibody to GBM. To minimize the background, we used normal human kidneys, as we have demonstrated that anti-GBM antibodies in our model also reacted with human GBM (16). Briefly, frozen sections of normal human kidney were incubated with the testing antibody for 2 h at 20°C and washed extensively. The section was incubated further with FITC-labeled goat anti-rat IgG or IgM antibodies (1:50; Southern Biotechnology) and viewed with a confocal microscope in a double-blind manner (FV 500; Olympus, Melville, NY). Confocal images were digitally recorded.

Purification of B Cell Population

Lymphocytes were isolated from different lymph nodes and adjusted to 10^7 cells/ml. B cells were purified with positive magnetic beads sorting following the manufacturer's instructions (MACS; Miltenyi Biotech Inc., Auburn, CA). Briefly, after preincubation with normal mouse IgG, the lymphocytes were incubated on ice with magnetic beads coated with mAb OX33 for 30 min and then added to the isolation column located in a magnetic field. The column was washed thoroughly with cold PBS, and B cells were eluted from the reverse direction in the absence of a magnetic field. The cell fractions were analyzed with flow cytometry after staining with PE-labeled OX33 and FITC-labeled anti-rat IgG/M. The purified B cells were used immediately for isolation of total RNA.

Reverse Transcription–PCR Detection of B Lymphocyte-Induced Maturation Protein Expression

Total RNA was isolated from lymph nodes or cell fractions at designated time points (Ambion, Austin, TX), and cDNA was synthesized using 0.1 μg of total RNA through a reverse transcription (RT) reaction (RNA PCR Core Kit; Applied Biosystems, Foster City, CA). PCR was used to detect B lymphocyte-induced maturation protein (*blimp*) mRNA using a pair of primers (5′-CCTTGCTACATGTGTGTCAGTTGG-3′, 5′-TGCTAGCATGTGTGGAATCTCTGG-3′), which resulted in a 400-bp product, under the following conditions: Preheating at 94°C for 3 min followed by 30 cycles (94°C for 60 s, 64°C for 30 s, 72°C for 60 s; GeneAmp9700; Applied Biosystems) (21). Expression of a housekeeper gene (glyceraldehyde-3-phosphate dehydrogenase) was used as an internal control following a previous published RT-PCR method, which resulted in a 238-bp product (22). The products were separated by electrophoresis in 1.5% agarose gel, stained with ethidium bromide, and visualized under ultraviolet light illumination. Selected samples were also used for real-time PCR following the identical conditions as described above. Briefly, after the RT reaction, cDNA concentrations were determined by a Microplate Spectrophotometer (SPECTRAmax; Molecular Devices, Sunnyvale, CA). Real-time PCR was carried out at two concentrations of the cDNA (1.5 ng/50 μl and 0.75 ng/50 μl) in duplicate in an iCycler iQ real-Time PCR detection system using iQ SYBR Green Supermix (Bio-Rad, Hercules, CA). Housekeeper gene glyceraldehyde-3-phosphate dehydrogenase was used as the standard. Relative abundance of *blimp-1* expression was calculated following the $2^{-\Delta\Delta C}{}_T$ method (23).

Results

Expansion of T and B Cells in RDLN of Rats with Anti-GBM GN

As the first step to investigate how anti-GBM antibodies were produced, we searched for the location of anti-GBM antibody production in the immunized WKY rats. Several previous studies have demonstrated the presence of B cells/extra-lymph node germinal center in the kidneys of several types of GN (24,25). We first examined the kidney-infiltrating leukocytes in pCol(28–40)-immunized WKY rats. The infiltrating leukocytes were isolated from either the interstitial tissue or glomeruli of diseased kidneys at two different stages (days 25 and 40 after immunization) and analyzed by flow cytometry (Figure 1). Although robust increases in several leukocyte populations, especially $CD4^+$ and $CD11b/c^+$ populations, were observed (data not shown), no significant number of $OX33^+/IgG/M^+$ cells (B cells) among the infiltrating leukocytes was detected at either stage (Figure 1B). Thus, the kidney was an unlikely location for anti-GBM antibody production.

We observed that a special lymph node in close proximity to the renal hilum, above the renal vein, of each diseased kidney was consistently enlarged in the immunized WKY rats after 25 to 35 d after immunization (Figure 2C). However, enlargement of the lymph nodes at the same location was not observed in CFA-immunized WKY controls (Figure 2B). In rats that were immunized with pCol34A, which has altered specificity of T cell epitope and nonpathogenic (see Table 1), enlargement of the lymph node was also not observed. Thus, enlargement of the lymph node was associated only with glomerular injury as well as anti-GBM antibody.

Using India ink as a tracer, lymphatic drainage of the renal cortex was investigated. It took 3 h for the ink to stain the first lymph node, which was in the identical location of the enlarged lymph node (Figure 2A). Microscopic observation showed accumulation of carbon particles in the cortex of the lymph node. Thus, the enlarged lymph node described above was the draining lymph node to the renal cortex. This lymph node was designated as RDLN. Quantitative analyses on the lymphocyte numbers from RDLN ranged from 31.5 up to 55×10^6 lymphocytes/node in pCol(28–40)-immunized WKY rats sampled at 35 to 40 d, as

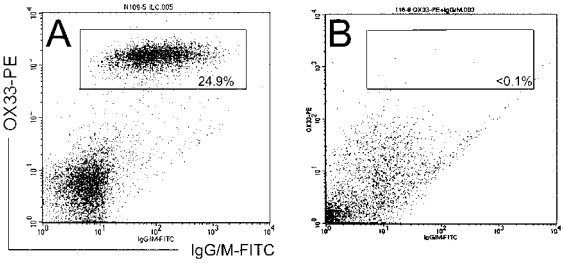

Figure 1. Flow cytometry demonstrates absence of $OX33^+$ IgG/M^+ B cells among the leukocytes infiltrating the diseased kidney of a Wistar Kyoto (WKY) rat that was immunized with pCol(28–40) at day 35. (A) Lymphocytes from the inguinal lymph node (ILN) of the same rat as the positive control show a $OX33^+IgG/M^+$ B cell population. (B) Leukocyte populations infiltrating the kidney; the cells are gated on forward scatter/side scatter for analysis; notice absence of $OX33^+IgG/M^+$ B cells.

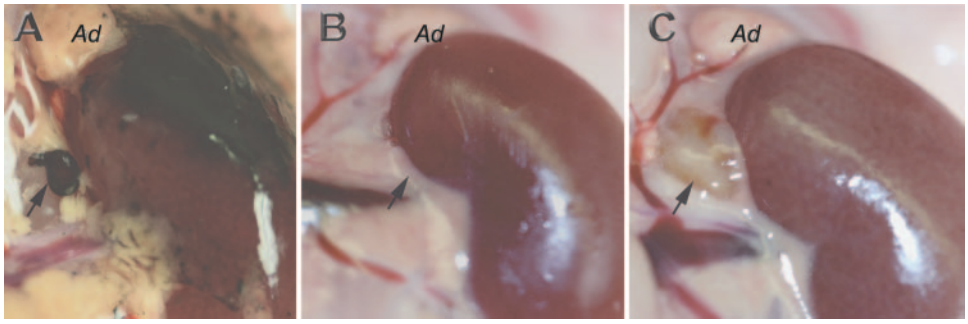

Figure 2. Enlargement of renal draining lymph node (RDLN) in WKY rats that were immunized with pCol(28–40). (A) India ink injection revealing a stained RDLN. (B) A normal RDLN in a complete Freund adjuvant (CFA)-immunized rat at day 35. (C) An enlarged RDLN in a pCol(28–40)-immunized rat at day 35. Arrows indicate RDLN. Ad, adrenal gland.

compared the range of 0.9 to 1.3 $\times$ 10^6/node in CFA controls at the same time. Flow cytometry further showed a significant expansion of $OX33^+$ B cells and $CD4^+$ cells in the enlarged RDLN (data not shown). Those results suggested that the enlarged RDLN probably was the location of anti-GBM antibody production.

B Cells in RDLN Produce Anti-GBM

We next asked whether B cells in enlarged RDLN of diseased kidneys were specific to GBM antigens. Lymphocytes were isolated from RDLN of WKY rats 35 d after immunization with pCol(28–40) for *in vitro* antibody production (Table 2). As an internal control, the cells that were isolated from ILN, to which the injected pCol(28–40) drained, were used. Lymphocytes that were isolated from RDLN or ILN of the rats that were immunized with pCol34A were used as additional controls. The lymphocytes from ILN of rats that were immunized with pCol(28–40) produced a significant amount of IgG (Table 2). ELISA demonstrated that the produced IgG showed strong antibody activity to pCol(28–40) (Table 2). However, the IgG that was produced by ILN cells, even when concentrated up to 50 μg/ml, failed to react with GBM by either ELISA or immunofluorescence (Figure 3A).

Conversely, the lymphocytes that were isolated from RDLN of only pCol(28–40)-immunized WKY rats produced a significant quantity of IgG (Table 2). The IgG that was produced by RDLN of pCol(28–40)-immunized WKY failed to react with pCol(28–40) as measured by ELISA (Table 2). However, indirect immunofluorescence demonstrated that the IgG that was produced by RDLN strongly reacted with native GBM at a concentration as low as 1 μg IgG/ml (Figure 3B). The IgG that was produced by RDLN also showed an unanticipated reactivity with nuclear antigens, suggesting the production of anti-nuclear antibodies in RDLN as well (Figure 3B). In contrast, only a trace amount of IgG was detected in RDLN from pCol34A-immunized WKY rats (Table 2). We concluded that RDLN of pCol(28–40)-immunized WKY rats was the location of autoreactive B cells that were specific to GBM antigens. IgM antibody to GBM was undetectable by indirect immunofluorescence or ELISA. Although anti-nuclear antibody was produced by RDLN B cells, circulating anti-nuclear antibody was not detected by indirect immunofluorescence.

Absence of pCol(28–40)-Specific B Cells in RDLN

To exclude any possible connections between GBM- and pCol(28–40)-specific B cells, we next analyzed the specificity of B cells in both the RDLN and ILN of pCol(28–40)-immunized WKY rats at day 20, when anti-GBM antibodies became detectable by

Table 2. In vitro production of antibodies from different sources of lymphocytes and their specificity to pCol(28–40) or GBM[a]

Cell Source	IgG (μg/4 $\times$ 10^7 Cells)	Antibody to pCol(28–40) ($O.D._{490nm}$)	Antibody to GBM	
			Immunofluorescence[b]	ELISA[c]
pCol(28–40)-immunized WKY				
ILN	3.71	0.977	−	0.009
RDLN	2.65	0.004	+++	0.253
pCol34A-immunized WKY				
ILN	3.27	0.702	−	−0.001
RDLN	0.92	−0.007	−	0.003

[a]Three independent experiments were performed, and only one experiment is shown; the other two have similar results. ILN, inguinal lymph nodes; RDLN, renal draining lymph node.
[b]For indirect immunofluorescence detection of anti-GBM antibodies, see Figure 3.
[c]IgG concentrations was adjusted to 10 ng/ml; the same concentration of normal rat IgG was used as control for background.

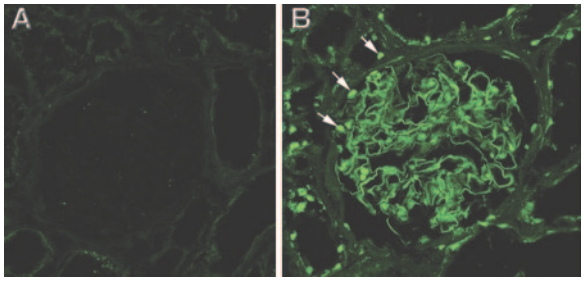

Figure 3. Immunofluorescence detection of antibodies to native glomerular basement membrane (GBM) that were produced by lymphocytes from ILN (A) or RDLN (B) of a pCol(28–40)-immunized WKY rat, sampled at day 35. Notice that antibodies from RDLN (B) react not only with GBM but also nuclear antigens (arrows).

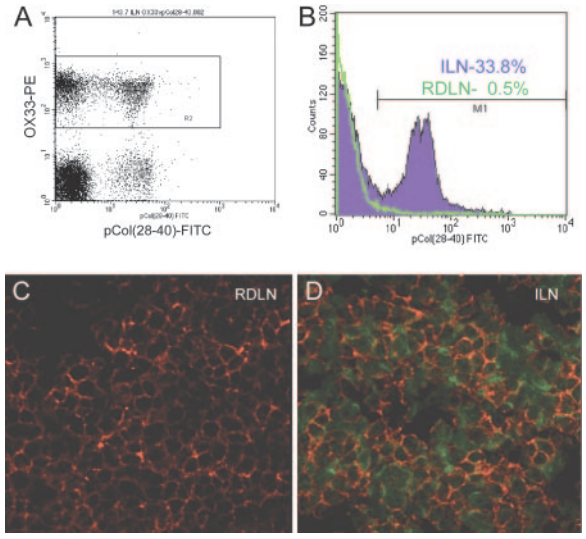

Figure 4. Absence of pCol(28–40)-specific B cells in RDLN of a pCol(28–40)-immunized WKY rat at day 20. (A) Flow cytometry on lymphocytes of ILN showing $OX33^+pCol(28–40)^-$ and $OX33^+pCol(28–40)^+$ B cell populations. (B) Histogram based on gated $OX33^+$ cells as shown in A; blue line, ILN; green line, RDLN; percentages of $pCol(28–40)^+$ cells among $OX33^+$ cells are indicated. (C and D) Confocal micrographs of immunofluorescence for detecting pCol(28–40)-specific B cells in the germinal center, stained with OX33-PE and FITC-pCol(28–40); notice that FITC-pCol(28–40) staining is absent in RDLN (C) but present in ILN; one germinal center is shown for each.

immunofluorescence. FITC-pCol(28–40) was used as a probe to identify pCol(28–40)-specific B cells (Table 1). FITC-pCol(28–40) bound to a population (approximately 12.2%) of cells that were isolated from ILN of pCol(28–40)-immunized WKY rats and accounted for approximately 33.8% of total $OX33^+$ B cells (Figure 4A). We also observed a population of $OX33^-pCol(28–40)^+$, which probably was anti-GBM plasma cells, which lost CD45R expression (26). Binding of FITC-pCol(28–40) to the B cells was specific, as nonlabeled pCol(28–40) could inhibit the binding. In contrast, only 0.1% of cells from RDLN of the same animals were stained as "positive" at day 20, and thus only $<0.5\%$ of B cells might be $pCol(28–40)^+$ cells (Figure 4B). This percentage was close to the background, which was set by lymphocytes from ILN of control rats that were immunized with CFA alone or from normal WKY. B cells that were specific to pCol(28–40) were present in RDLN at a much later stage (day 35; 6.8%). A slightly higher percentage of pCol(28–40)-specific B cells (7.5%) were also observed in other lymph nodes, such as axillary nodes, which were more distant from ILN. Those results suggested that presence of pCol(28–40)-specific B cells in RDLN at a later stage probably was due to secondary migration of antigen-specific B cells throughout the lymphatic system. We concluded that pCol(28–40)-specific B cells were not present in RDLN.

Absence of pCol(28–40)-specific B cells in the RDLN was also confirmed by two-color immunofluorescence (Figure 4, C and D). RDLN and ILN were sampled from the same rats at day 20 after immunization. Both lymph nodes displayed well-developed germinal centers (GC) with organized $OX33^+$ B cells. Binding of FITC-pCol(28–40) to the B cells in many GC was observed in ILN (Figure 4D). In contrast, FITC-pCol(28–40) failed to bind to B cells in any GC in RDLN (Figure 4C). Those results supported our earlier observation that RDLN of pCol(28–40)-immunized rats lacked pCol(28–40)-specific B cells.

Timing for Activation of B Cells in RDLN

To estimate when the B cells, specific to either pCol(28–40) or native GBM in ILN or RDLN, were activated, we established a time course of antibody response, as well as of glomerular injury, in pCol(28–40)-immunized WKY rats (Figure 5). Prominent glomerular injury was histologically observed at day 20 after immunization and rapidly developed into crescentic lesions/tuft necrosis in 100% of glomeruli after day 30 (Figure 5A). However, our previous study showed that significant proteinuria developed in the immunized rats at approximately 15 to 18 d, suggesting the occurrence of subhistologic damage in the GBM (16).

IgG-type circulating antibodies to the peptide pCol(28–40) became detectable as early as day 8, and its titer elevated rapidly after day 12. The circulating antibodies reached a plateau at day 20 and persisted at this level during the entire experimental period (Figure 5B). However, direct immunofluorescence showed a positive GBM-bound IgG antibody in 37% of the rats at day 20. At day 25, most (75%) of rats showed positive in the binding of antibody to GBM. After day 30, the binding of antibody to GBM became extremely intensive in most of the rats (Figure 5C). IgG circulating antibodies to GBM, however, were not detectable by either ELISA or indirect immunofluorescence (Figure 5B). On the basis of the comparisons between antibodies and glomerular damage, we concluded that production of anti-pCol(28–40) antibodies significantly preceded the glomerular injury, but production of anti-GBM antibodies occurred after the glomerular injury. Thus, there was a significant time gap between production of anti-pCol(28–40) antibodies in ILN and anti-GBM antibodies in RDLN. Those data also suggested that that T cell–mediated glomerular damage was a prerequisite for production of anti-GBM antibodies in the immunized rats.

For confirming the time gap between B cell activation in the two lymph nodes, expression of *blimp-1*, which is associated with B cell

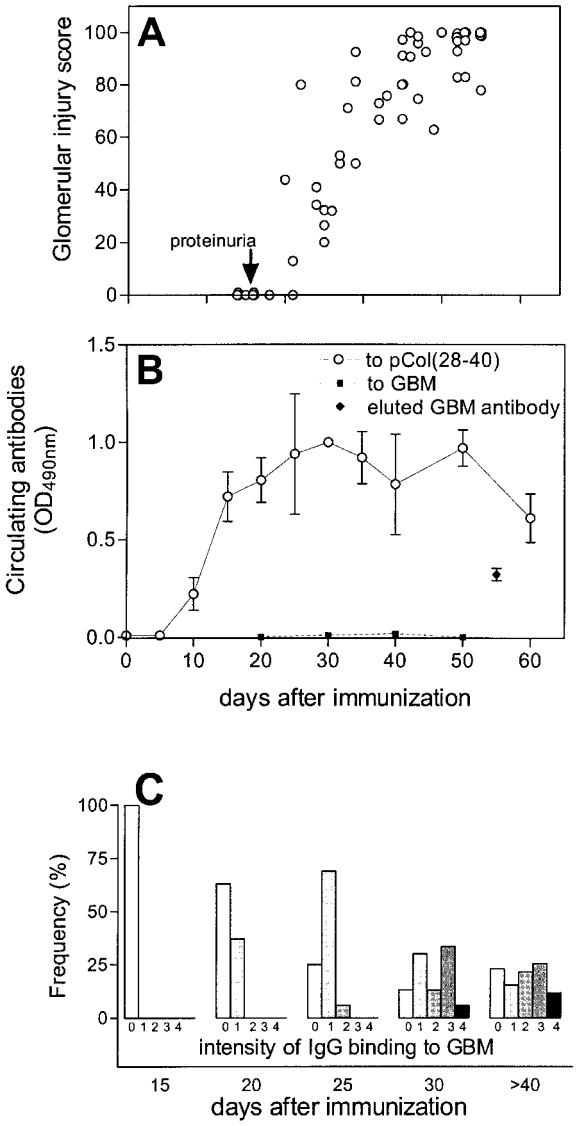

Figure 5. Time courses of renal pathology and antibody response in WKY rats that were immunized with pCol(28–40). (A) Renal pathology expressed as a glomerular injury score; each dot represents one individual; time for beginning of proteinuria is indicated by an arrow. (B) Circulating antibodies to pCol(28–40) (○) and GBM (●) as measured by ELISA; antibody to native GBM, eluted from diseased glomeruli, was used as a positive control (◆); ≥3 samples for each time point. (C) IgG GBM antibodies, expressed as frequency of the intensity (0 to 4) of direct immunofluorescence on GBM, at different time points; samples (>10) in each group were taken from the indicated time ± 2 d.

activation and plasma cell differentiation (21), in RDLN and ILN was investigated by RT-PCR. Expression of *blimp-1* became detectable in the ILN as early as day 5 and elevated to a high level from day 10 to day 30. Its expression then declined to a medium level at day 35 (Figure 6A). In contrast, *blimp-1* expression in RDLN was only slightly above the background level (lymphocytes from nonimmunized rats) at day 10 and detectable at a medium level at day 19. Its expression in RDLN reached a high level especially at day 35 (Figure 6A). Real-time quantitative PCR revealed a >40-fold increase in *blimp-1* expression levels in RDLN between days 19 and 35. Using magnetic bead sorting, B cells were purified from RDLN lymphocytes (Figure 6B). The $OX33^+$ B cell fraction showed a high level of *blimp* expression, whereas $OX33^-$ cells showed no expression of *blimp* (Figure 6C). Thus, detected *blimp* expression originated from the B cells. This experiment again demonstrated that B cell activation in RDLN occurred at a much later stage than that in ILN.

Discussion

Presence of anti-GBM antibody is the hallmark of Goodpasture's syndrome, or anti-GBM GN. The precise mechanism by which autoantibodies to diverse GBM antigens are produced remains unclear. We have established a rat model for anti-GBM GN in which the nephritogenic T cell epitope pCol(28–40), derived from Goodpasture's antigen collagen IV α3 chain, not only induces glomerular injury but also can elicit anti-GBM autoantibodies (15). Our studies strongly argue that B cell epitope spreading probably occurs during glomerular damage, which leads to GBM antibody production. In this study, we further identified RDLN as the location of the autoreactive B cell activation. Thus, diverse GBM-specific B cell populations can be tracked and studied. This unique feature will greatly facilitate our investigations on the precise mechanism of GBM antibody production. We believe that our investigation will also contribute to our understanding of the mechanism of GBM antibody production as well as B cell epitope spreading.

Activation of GBM-Specific Autoreactive B Cells in RDLN

The most significant finding in this study is identification of RDLN as the specific location where the autoreactive B cells to GBM and nuclear antigens are activated. The most direct evidence

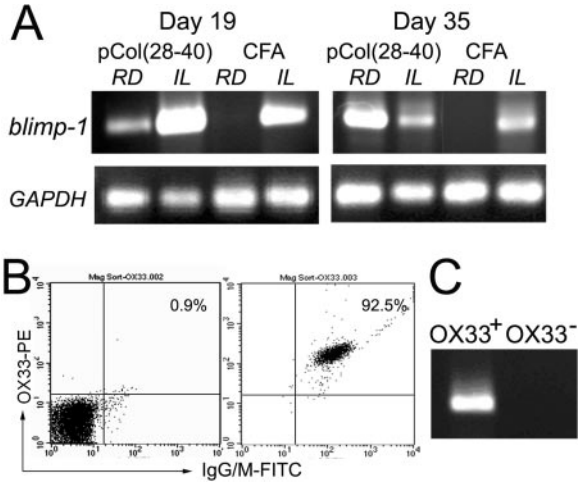

Figure 6. Reverse transcription–PCR detection of expression of B lymphocyte-induced maturation protein (*blimp-1*) in RDLN (RD) or ILN (IL) of pCol(28–40)-immunized WKY or CFA control (A). Expression of housekeeper gene glyceraldehyde-3-phosphate dehydrogenase is also shown. (B) Flow cytometry of $OX33^-$ and $OX33^+$ cells after magnetic bead sorting. (C) *Blimp-1* expression in sorted $OX33^+$ or $OX33^-$ populations.

came from *in vitro* antibody production experiments. IgG that was produced only by RDLN B cells showed strong antibody activity to native GBM.

Indirect evidence also supported our conclusion. T cell epitope pCol(28–40) also contains a peptide-specific B cell epitope (16) (Table 1). Because antibodies to this B cell epitope do not react with native GBM, this peptide-specific B cell epitope has served as an excellent internal control, which has allowed us to observe simultaneously activation of two B cell populations with different specificities. Using synthetic FITC-pCol(28–40), we were able to detect or locate quantitatively pCol(28–40)-specific B cell populations. We first demonstrated, at either day 20 or day 35, the presence of a large percentage of pCol(28–40)-specific B cells in the ILN, to which immunized pCol(28–40) drained. In contrast, pCol(28–40)-specific B cells were not present in RDLN at an earlier stage (day 20), when anti-GBM antibodies had become detectable. Therefore, the expanding B cell populations in RDLN and ILN were different in their specificity: Those in ILN were pCol(28–40) specific, whereas those in RDLN were not. Although we still lack a method to detect directly GBM-specific B cells, we are able to conclude that expanding B cells in RDLN were GBM or nuclear antigen specific. A small percentage of pCol(28–40)-specific B cells was observed in RDLN at a later stage (day 35). Because a similar percentage of peptide-specific B cells were also seen in distant lymph nodes such as the axillary node, it is reasonable to conclude that this B cell population is not specifically expanded in RDLN but probably is a result of the secondary migration of B cells throughout the lymphatic system.

Our time-course study showed that production of anti-GBM antibodies occurred after T cell–mediated glomerular injury. In contrast, production of antibodies to pCol(28–40) preceded glomerular injury. By tracking B cells in RDLN, we were able to determine more precisely when the GBM-specific B cells were activated. *Blimp-1* is a transcription factor that is involved in differentiation of plasma cells (21). Delayed expression of *blimp* in B cells from RDLN also indicates that GBM-specific B cells were activated after glomerular injury. Those results suggest that glomerular injury may be a prerequisite for activation of GBM-specific B cells.

Our Model Is a Unique Tool for Studying B Cell Epitope Spreading

Production of autoantibodies is characteristic of autoimmune diseases mediated by either an antibody or a T cell mechanism. It has been a hot topic in immunology to understand mechanisms by which autoreactive B cells are activated. Sophisticated BcR transgenic models have been instructive in our understanding of the mechanism of B cell tolerance, especially in T independent responses. However, mono-specific B cell populations limit their value for studying the mechanism of a diversified autoantibody response, which is more frequently seen among human autoimmune diseases (1). How to track diverse B cell populations is a key to determining how autoreactive B cells are activated especially in T cell–mediated autoimmune diseases.

Our model provides an excellent tool to address this issue. First, our model for anti-GBM disease is a typical autoimmune disease model with production of anti-GBM antibody. Second, identification of the location of autoreactive B cell activation, *i.e.*, RDLN, will allow us to study the activation of autoreactive B cells after T cell–mediated tissue damage at cellular and molecular levels without genetic manipulation. Third, a unique peptide-specific B cell epitope in pCol(28–40) is an excellent internal control. It allows us to compare the B cell response to an immunizing "foreign" B cell epitope *versus* autoantigens released from T cell–mediated tissue injury. Fourth, we recently found that Lewis rats possess identical MHC to WKY. Although Lewis rats are able to mount an identical T cell response to pCol(28–40), they do not develop anti-GBM disease or anti-GBM antibodies. Thus, Lewis rats will provide an essential control for our investigation on the factors beyond the T cell mechanism that determines B cell epitope spreading. Finally, many models for glomerular injury are mediated by mechanisms other than autoimmunity (27–29). Those models will help us to answer why only autoreactive T cell–mediated glomerular injury leads to activation of autoreactive B cells.

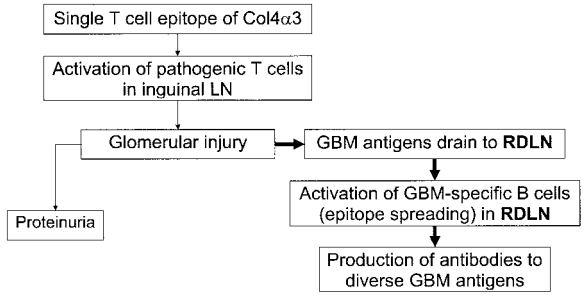

Figure 7. Schematic diagram describes the hypothetic mechanism by which antibodies to diverse GBM antigens are produced after immunization with a single nephritogenic T cell epitope in our model. Bold arrows indicate the steps that are based on the findings described in this article.

Hypothesis: How Antibodies to Diverse GBM Antigens Are Produced

It has been well demonstrated that GBM patients usually produce autoantibodies to multiple GBM epitopes or proteins. On the basis of our findings in both this and previous articles, we are able to propose a general hypothetical mechanism by which diverse GBM antibodies are produced in our model (Figure 7) (30). First, a single pathogenic T cell epitope activates T cells, which cause glomerular inflammation and GBM damage. Second, damage of GBM not only leads to proteinuria but also results in release of GBM antigens, which drain to RDLN. Finally, B cells specific to GBM antigens are activated in RDLN and begin to produce diverse GBM antibodies, which eventually bind to native GBM. Thus, a single T cell epitope triggers a full clinical spectrum of anti-GBM glomerulonephritis: Proteinuria, glomerular damage, and diverse GBM antibodies.

Acknowledgments

This study was supported by the National Institutes of Health (NIH) grant RO1 DK60029 (Y.H.L). J.R. is a graduate student supported by NIH T32DE015355. L.T. is supported by NIH DK60029-03S1. C.Z. is a postdoctoral trainee supported by NIH T32 HD07324. Histology support was provided by the Histology Core Laboratory, Dental Branch,

the University of Texas Health Science Center at Houston. Confocal microscopic images were provided by the Core Facilities at M.D. Anderson Cancer Center, University of Texas.

References

1. Boitard C: The spectrum of autoantibody in organ-specific autoimmune diseases. In: *B Cells and Autoantibody Production in Autoimmune Diseases.* New York, Chapman & Hall, 1996, pp 7–80
2. Wieslander J, Bygren P, Heinegard D: Isolation of the specific glomerular basement membrane antigen involved in Goodpasture syndrome. *Proc Natl Acad Sci U S A* 81: 1544–1548, 1984
3. Hellmark T, Johansson C, Wieslander J: Characterization of anti-GBM antibodies involved in Goodpasture's syndrome. *Kidney Int* 46: 823–829, 1994
4. Kefalides NA, Ohno N, Wilson CB: Heterogeneity of antibodies in Goodpasture syndrome reacting with type IV collagen. *Kidney Int* 43: 85–93, 1993
5. Savige JA, Gallicchio M, Georgiou T, Davies DJ: Diverse target antigens recognized by circulating antibodies in anti-neutrophil cytoplasm antibody-associated renal vasculitis. *Clin Exp Immunol* 82: 238–243, 1990
6. Fagarasan S, Honjo T: T-Independent immune response: New aspects of B cell biology. *Science* 290: 89–92, 2000
7. Danzer CP, Collins BE, Blixt O, Paulson JC, Nitschke L: Transitional and marginal zone B cells have a high proportion of unmasked CD22: Implications for BCR signaling. *Int Immunol* 15: 1137–1147, 2003
8. Mecklenbrauker I, Saijo K, Zheng NY, Leitges M, Tarakhovsky A: Protein kinase Cdelta controls self-antigen-induced B-cell tolerance. *Nature* 416: 860–865, 2002
9. Goodnow CC: Transgenic mice and analysis of B-cell tolerance. *Annu Rev Immunol* 10: 489–518, 1992
10. Chen C, Nagy Z, Radic MZ, Hardy RR, Huszar D, Camper SA, Weigert M: The site and stage of anti-DNA B-cell deletion. *Nature* 373: 252–255, 1995
11. Lou YH, Tung KS: T cell peptide of a self-protein elicits autoantibody to the protein antigen. Implications for specificity and pathogenetic role of antibody in autoimmunity. *J Immunol* 151: 5790–5799, 1993
12. Milich DR, McLachlan A, Raney AK, Houghten R, Thornton GB, Maruyama T, Hughes JL, Jones JE: Autoantibody production in hepatitis B e antigen transgenic mice elicited with self T-cell epitope and inhibited with nonself peptide. *Proc Natl Acad Sci U S A* 88: 4348–4352, 1994
13. James JA, Gross T, Scofield RH, Harley JB: Immunoglobulin epitope spreading and autoimmune disease after peptide immunization: Sm B/B'-derived PPPGMRPP and PPPGIRGP induce spliceosome autoimmunity. *J Exp Med* 181: 453–461, 1995
14. Topfer F, Gordon T, McCluskey J: Intra- and intermolecular spreading of autoimmunity involving the nuclear self-antigens La (SS-B) and Ro (SS-A). *Proc Natl Acad Sci U S A* 92: 875–979, 1995
15. Wu J, Arends J, Borillo J, Zhou C, Merszei J, McMahon J, Lou YH: A self T cell epitope induces Autoantibody response: Mechanism for production of antibodies to diverse glomerular basement membrane antigens. *J Immunol* 172: 4567–4574, 2004
16. Wu J, Borillo J, Glass II WF, Hicks J, Ou CN, Lou YH: T cell epitope of glomerular basement membrane antigen induces severe glomerulonephritis. *Kidney Int* 64: 1292–1301, 2003
17. Wu J, Hicks J, Borillo J, Glass II WF, Lou YH: CD4+ T cells specific to a glomerular basement membrane antigen mediate glomerulonephritis. *J Clin Invest* 109: 517–524, 2002
18. Robertson J, Wu J, Arends J, Glass Ii W, Southwood S, Sette A, Lou YH: Characterization of the T-cell epitope that causes anti-GBM glomerulonephritis. *Kidney Int* 68: 1061–1070, 2005
19. Gordon T, Topfer F, Keech C, Reynolds P, Chen W, Rischmueller M, McCluskey J: How does autoimmunity to La and Ro initiate and spread? *Autoimmunity* 18: 87–92, 1994
20. Tung KS, Lou YH, Garza KM, Teuscher C: Autoimmune ovarian disease: Mechanism of disease induction and prevention. *Curr Opin Immunol* 9: 839–847, 1998
21. Turner CA, Mack DH Jr, Davis MM: Blimp-1, a novel zinc finger-containing protein that can drive the maturation of B lymphocytes into immunoglobulin-secreting cells. *Cell* 77: 297–306, 1994
22. Hohnel K, Dietz R, Willenbrock R: Quantification of low abundance natriuretic peptide receptor mRNA in rat tissues. *Clin Chem Lab Med* 37: 805–812, 1999
23. Livak KJ, Schmittgen TD: Analysis of relative gene expression data using real-time quantitative PCR and the 2(-Delta Delta C(T)) method. *Methods* 25: 402–408, 2001
24. Peterson KS, Huang JF, Zhu J, D'Agati V, Liu X, Miller N, Erlander MG, Jackson MR, Winchester RJ: Characterization of heterogeneity in the molecular pathogenesis of lupus nephritis from transcriptional profiles of laser-captured glomeruli. *J Clin Invest* 113: 1722–1733, 2004
25. Lenda DM, Stanley ER, Kelley VR: Negative role of colony-stimulating factor-1 in macrophage, T cell, and B cell mediated autoimmune disease in MRL-Fas(lpr) mice. *J Immunol* 173: 4744–4754, 2004
26. Lin KI, Tunyaplin C, Calame K: Transcriptional regulatory cascades controlling plasma cell differentiation. *Immunol Rev* 194: 19–28, 2003.
27. Fujigaki Y, Yousif Y, Morioka T, Batsford S, Vogt A, Hishida A, Miyasaka M: Glomerular injury induced by cationic 70-kD staphylococcal protein; specific immune response is not involved in early phase in rats. *J Pathol* 184: 436–445, 1998
28. Fujihara CK, De Nucci G, Zatz R: Chronic nitric oxide synthase inhibition aggravates glomerular injury in rats with subtotal nephrectomy. *J Am Soc Nephrol* 5: 1498–1507, 1995
29. Hruby ZW, Lowry RP, Forbes RD, Blais D: Mechanisms of glomerular injury in experimental immune nephritis. II. Effect of a platelet activating factor receptor antagonist in an autologous nephritis model. *Arch Immunol Ther Exp* 39: 575–586, 1991
30. Lou YH: Anti-GBM glomerulonephritis: A T cell mediated autoimmune disease? *Arch Immunol Ther Exp* 52: 96–103, 2004